Available online at www.sciencedirect.com
SCIENCE DIRECT
Polymer 46 (2005) 3175–3184
polymer
www.elsevier.com/locate/polymer

Monte Carlo simulation of microemulsion polymerization

Lixing Nie, Wuli Yang, Hongdong Zhang*, Shoukuan Fu*

Department of Macromolecular Science, Key Laboratory of Macromolecular Engineering of Polymers of Ministry of Education, Fudan University, Shanghai 200433, People's Republic of China

Received 14 October 2004; received in revised form 17 January 2005; accepted 19 January 2005
Available online 4 March 2005

Abstract

Monte Carlo simulation of chemically reacting systems based on the master equation was used to describe the stochastic time evolution of the microemulsion polymerization system. A model was developed to demonstrate its applicability for hexyl methacrylate and styrene microemulsion polymerization. The properties of final latex, such as the particle size and molecular weight distributions were obtained simultaneously. The polymerization behavior and properties of final latexes were well reproduced. The model is valuable in confirming or elucidating the various mechanisms in the polymerization. The entry and desorption mechanism was well established to account for the polymerization kinetics. The general polymerization behavior of hydrophobic monomer in microemulsions was properly simulated by the model proposed.

Keywords: Simulation; Microemulsion polymerization; Monte Carlo

1. Introduction

Microemulsion polymerization is an interesting class of compartmentalized polymerization reactions that produce nanoscale polymer latexes with high molecular weights, which have many potential applications [1,2]. It is important to be able to predict and control the kinetics, particle size and molecular weight distributions of these latexes. However, there have only been a few attempts at modeling the reaction kinetics and molecular weight and particle size distributions [3–6]. Such complex reaction schemes require consideration of many physical and chemical processes. For most of these processes, many model conceptions are found in the literature [7–9].

Guo et al. [3,7] developed a thermodynamic partitioning model to count the monomer concentration in particles during styrene microemulsion polymerization and a mathematical model to simulate the polymerization kinetics, which is in agreement with experimental conversion data up to 80% conversion in some cases, while failing to describe the concentration of particles above about 35% conversion.

Morgan and Kaler [4] have developed a rather simple mechanistic model to describe the polymerization kinetics of hexyl methacrylate (HMA) in microemulsions prepared with a mixture of the surfactants dodecyltrimethylammonium bromide (DTAB) and didodecyldimethylammonium bromide (DDAB). The particle size and molecular weight distributions (PSDs and MWDs) derived from this model assuming full exit of transfer-generated monomeric radical agree with the experimental results from small-angle neutron scattering (SANS) measurement [10,11]. However, the equations derived to describe the time-evolution of the PSD and MWD are rather complex and only applied to idealized cases. The model's extensions provide insight into the effect of nonlinear monomer partitioning, nonnegligible bimolecular termination and diffusion limitations to propagation [5,12,13].

An elaborate model for the kinetics of microemulsion polymerization has been proposed by Mendizabal et al. [6]. This model predicts a large desorption rate and the occurrence of both homogeneous and micellar nucleation mechanisms to account for the continuous nucleation of particles. This scheme contained four independent variables whose values are not well established, and so the utility of this model for rigorous mechanistic hypothesis testing is compromised.

* Corresponding authors.
E-mail addresses: zhanghd@etang.com (H. Zhang), skfu@fudan.edu.cn (S. Fu).

0032-3861/$ - see front matter © 2005 Elsevier Ltd. All rights reserved.
doi:10.1016/j.polymer.2005.01.085

In order to achieve a better mechanistic understanding of polymerization in these microemulsions, Monte Carlo methods were used to simulate the polymerization behavior. A simple scheme was developed based on simplified mechanism according to Morgan–Kaler's model [4]. The simulation is capable of reproducing the kinectic behavior and particle size distribution, which are perfectly identical with the theoretical calculation. Consequently, we developed a more realistic model for microemulsion polymerization suited for hexyl methacrylate and styrene system, which is valuable in confirming or elucidating the various mechanisms in the polymerization. The entry and desorption mechanism was well established to account for the polymerization kinetics.

2. Models description

2.1. Algorithm for Monte Carlo simulation

The stochastic method described by Gillespie [14] has proven to be a useful technique for studying the kinetics and MWDs in free-radical polymerization [15,16] and living free-radical polymerization (LFRP) [17] and other complex chemical reactions [18,19]. The convenience and feasibility of the stochastic Monte Carlo algorithm have been demonstrated when it has been used for pulsed laser, or rotating sector, initiated radical polymerization, with or without chain transfer reactions [15,16] and LFRP with one or two-component initiating systems [17]. More recently, Monte Carlo method has been used to reveal the best reactivity ratio of active centers of inimer or multifunctional initiator to narrow MWD or achieve highest degree of branching in self-condensing vinyl polymerization with unequal rate constants [20]. Also, a random sampling technique combined with a Monte Carlo method was used to simulate the branching process of polypropylene to find the relationships between the branching parameter and the melt flow rate, on the one hand, and the molecular weight, on the other [21]. Especially in the case of very complex reaction schemes such as microemulsion polymerization where conventional methods require a high level of sophistication and include many simplified assumptions, Monte Carlo methods seem to be a simple and flexible alternative. These kinds of methods are based on the definition of reaction probabilities. With these probabilities and random numbers, the fate (with respect to its reaction behavior) of a specific amount of reactant molecules is simulated.

The details of the algorithm were given in Ref. [15]. In order to keep the integrity of this paper, here we briefly review this algorithm.

A small part of the overall reaction volume is picked out

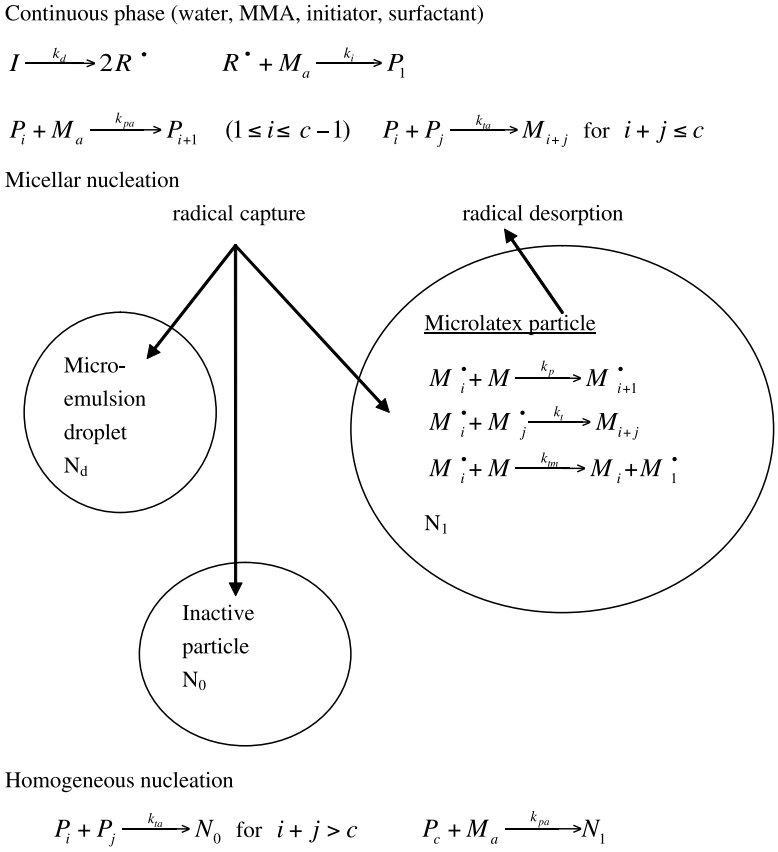

Scheme 1.

to be a suitable simulation space, which provides most of the information. Suppose the volume V contains a spatially homogeneous mixture of N chemical species which can interact through M specified chemical reaction channels. The kind of reaction μ that will happen in a time interval $(t+\tau \rightarrow t+\tau+\Delta\tau)$ is determined by a unit-interval uniformly distributed random number, r_1, according to the following relation:

$$\sum_{\nu=1}^{\mu-1} R_\nu < r_1 \sum_{\nu=1}^{M} R_\nu \leq \sum_{\nu=1}^{\mu} R_\nu \tag{1}$$

where R_ν is the rate of νth reaction per molecule in the simulation volume. The time interval between two successive reactions,τ is a stochastic variable determined by a unit-interval, uniformly distributed random number, r_2,

$$\tau = \frac{1}{\sum_{\nu=1}^{M} R_\nu} \ln\left(\frac{1}{r_2}\right) \tag{2}$$

2.2. Model for microemulsion polymerization

The basic sequence of events has been widely accepted to describe the general mechanism of o/w microemulsion polymerization. Once an initiator is added to a one-phase thermodynamically stable system comprised of microemulsion droplets (swollen micelles) dispersed in the continuous phase, the polymerization begins. Radicals are generated in the aqueous phase by initiator decomposition and enter the microemulsion droplets, possibly with mediating aqueous phase propagation to reach a critical degree of polymerization and become amphiphilic enough before entering as proposed in the Maxwell–Morrison entry model for emulsion polymerization [8]. Upon entering, the chain continues to grow by consuming the monomer inside the particle and transport of system components occur simultaneously which determined by thermodynamics. Termination of a growing chain can occur by either biradical termination or chain transfer. Transfer generated radical may either continue to propagate in the same particle, be passed to another particle by a coalescence event, or exit to the aqueous phase where it may either terminate with another radical or enter another particle and continue propagating. Radicals propagating to critical length before entering can precipitate and cause homogeneous nucleation. Accordingly, the reaction scheme in the simulation is designed and shown in Scheme 1.

There are three types of microspheres viz. microdroplets, inactive particles and active particles. Once a radical enters, a microdroplet turns into an active particle, an inactive particle into an active particle, and an active particle into an inactive particle due to instantaneous termination. The reaction rates for entry and desorption are:

$$R_c = k_c R\, N \quad R_{des} = k_{des} N_1$$

where k_c, k_{des} are rate constants for entry and desorption, the value will be discussed later. R is concentration of aqueous phase radicals, N represents the number of particles of each type, and N_1 is the density of particles with small radicals, which can desorb.

To illustrate the algorithm suitable for microemulsion polymerization, we compare our numerical results with the analytical results obtained from Morgan–Kaler's model which ignore bimolecular termination either in the aqueous phase or in the particles. According to their model, there are five competitive events can occur in the system, which are initiator decomposition and radical propagation in the aqueous phase, radical capture by microemulsion droplets quickly and propagation in particles, active chains transfer to monomer and then exit from particles immediately. Due to fast capture of aqueous phase free radicals as assumptions in Morgan–Kaler's model, propagation in aqueous is rare events before entry, and radical capture is a fast process viz. not rate-determined.

It is straightforward to account for virtually any kinetic event and the desorption of oligomeric radicals was introduced to develop a more realistic model to simulate microemulsion polymerization of styrene and hexyl methacrylate, the following assumptions were made: (1) particles are generated by capture of radicals in aqueous phase by microemulsion droplets; (2) the polymer particles contain at most one growing radical due to instantaneous termination in particles; (3) only small radicals (either chain-transfer generated or initiator derived) undergo desorption; (4) the concentrations of monomer in the aqueous phase, particles and microemulsion droplets are in thermodynamic equilibrium owing to fast mass transport. We treat phase-transfer events like entry and exit of radicals as kinetic events.

2.2.1. Monomer partitioning

Since there are no independent measurements of the monomer concentration in the polymer particles during microemulsion polymerization, many efforts have been made to quantify monomer concentration in particles (C_p) through thermodynamic equilibrium partitioning [6,7]. As discussed by Kaler et al. [13], since the total area of surfactant monolayer of particles and micelles combined remains constant during microemulsion polymerization reaction, the surface energy does not play a role for monomer partitioning. The swelling of the polymer particles is opposed by the curvature energy of the surfactant monolayer of micelles and favored by the Flory–Huggins bulk polymer free energy. For good approximate and simplification, instead of using thermodynamic model the empirical formula is used to describe the evolution of C_p, which is linear decay, coincident with the thermodynamic model result for microemulsions those initial compositions are far away from the phase boundary, and is exponential decay for those close to the phase boundary.

2.2.2. Rate coefficient for radical desorption

It has been pointed out that radical desorption from the

polymer particles and micelles play an important role in particle formation [9] and biradical termination in particles [5]. In our simulation, it was assumed that small radicals include chain-transfer generated monomeric radicals and initiator derived radicals with no more than one monomer unit can desorb from the polymer particles or microemulsion droplets competing propagation in them. Once these radicals desorb, they participate aqueous phase reaction or reabsorption. In our simulation, k_{des} is the rate of diffusion of small radicals out of the particles, the expression for k_{des} as derived by Nomura is [22]:

$$k_{des} = \frac{12D_w/m_d d_P^2}{1 + 2D_w/m_d D_P} \tag{3}$$

where D_w and D_p are the diffusion coefficients of monomer radicals in the aqueous phase and the polymer particles, respectively, m_d is the partition coefficient of monomer radicals between the particles and the aqueous phase, and d_P is the diameter of the particles. Since particle diameter does not change much during microemulsion polymerization, to a first approximation we adopt a constant k_{des} throughout the polymerization.

2.2.3. Rate coefficients for radical entry

We assumed the same rate constant for radical capture by micelles and particles since in the present of so much surfactant the polymer particles are most likely fully covered with surfactant and hence are just as highly charged as the micelles. As suggested by Kaler [5], radical capture by micelles and eventually becoming an particle represents the entire sequence of events up to the first propagation step in a monomer-swollen micelle, which is a slow process, while radical capture by polymer particles is a fast process of instantaneous termination.

3. Results and discussion

3.1. Compared with Morgan–Kaler's mode for HMA system

Morgan–Kaler's model predicts conversion evolution with time according to Eq. (4), reaction rate according to Eq. (5),

$$f = 1 - \exp(-1/2At^2) \tag{4}$$

$$\frac{df}{dt} = Ate^{-1/2At^2} \tag{5}$$

where,

$$A = \frac{2k_d k_p C_0[I]}{M_0} \tag{6}$$

where k_d is initiator decomposition rate constant, k_p is the propagation rate constant, M_0 and $[I]$ are the initial macroscopic concentration of monomer and the initiator concentration in moles per liter of microemulsion, respectively, C_0 is an initial monomer concentration in the particles at the point at which sufficient polymer has formed to absorb all available monomer. As described in Section 2, k_c value was chosen large enough not to retard the polymerization rate. Microdroplet concentration was 2.1×10^{-3} M [4]. Using the same parameter (shown in Table 1), choosing 1.0×10^{-14} L as simulated volume, the kinetics of the polymerization of HMA microemulsion were simulated as shown in Figs. 1 and 2. The solid curve is calculated from Eq. (4) (shown as Theory). The simulated results agree completely with theoretical calculation.

The particle size distribution (PSD) will be obtained simultaneous during the simulation. The PSD results of Kaler's deducing [10] and our simulation with different initiator concentration (shown in Fig. 3) and at different conversion during polymerization (shown in Fig. 4) were quantitatively identical. This is a direct proof that stochastic simulation can apply to microemulsion polymerization, and the method used to deal with the system is reasonable.

3.2. The model for microemulsion polymerization

Based on the framework we developed for Morgan–Kaler's model, the desorption of oligomeric radicals was introduced to develop a more realistic model to simulate microemulsion polymerization of styrene and hexyl methacrylate as describe in Section 2. To get a better understanding about the model, the following considerations with

Table 1
Values of kinetic and physicochemical parameters used in simulation

Parameter	HMA [4][a]	Styrene [3][b]
Rate constant ($M^{-1}\,s^{-1}$)	k_p=995 $k_d=2\times10^{-5}$ k_{tr}=0.03 [10]	k_p=329 $k_d=4.4\times10^{-5}$ k_{tr}=0.006[c]
Water solubility (mM)	0.4 [5]	4.6 [5]
Monomer concentration (M)	0.257	0.466
Microdroplet concentration (mM)	2.1	7.6
Simulated volume (L)	1.0×10^{-14}	5.0×10^{-15}

[a] The values in the column without reference are form Ref. [4].
[b] The values in the column without reference are form Ref. [3].
[c] Between the value adopted in Ref. [3,5].

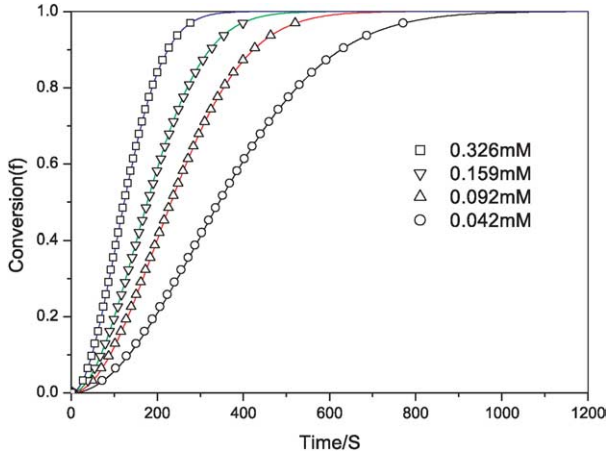

Fig. 1. Simulated conversion vs. time for the microemulsion polymerization of HMA with different V-50 initiator concentration. Solid lines are results from Eq. (4) and dots are simulated results using the same parameter values: $C_0=1.8$ M, $k_d=2\times10^{-5}$ s^{-1}, $k_p=995$ M^{-1} s^{-1}, $M_0=0.257$ M and $k_{tr}=0.01$ M^{-1} s^{-1}.

respect to the sensitive analysis of the parameters might be useful.

3.2.1. The effect of rate constants for entry and desorption

In order to guarantee the validity of our results, it is important to choose proper parameters in our simulations. However, the rate coefficients for radical entry and desorption are experimentally unavailable, it is necessary to give a detail examination on simulation results for different rate coefficients. For all initiator concentration adopted here, the effects of rate constant values on kinetic behaviors are the same trends. So we select $[I]=0.27$ mM case in Ref. [3] to discuss their influence. Here simulation volume was chosen as 5.0×10^{-15} L and good statistical properties can still be obtained. Other parameters are shown in Table 1.

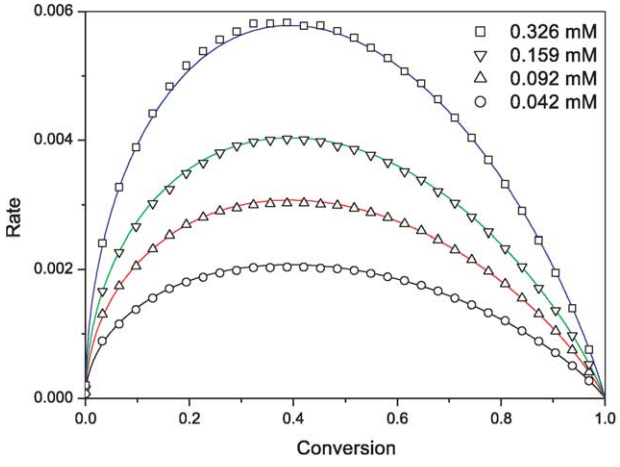

Fig. 2. Simulated rate vs. conversion (dots) for the microemulsion polymerization of HMA with different V-50 initiator concentration. Solid lines are results from Eq. (5) and dots are simulated results using the same parameter values as Fig. 1.

3.2.1.1. Rate coefficients for radical entry. Fig. 5 depicts the effect of the radical capture rate constant, k_c, on the kinetics of polymerization. As k_c increased, the polymerization rate becomes more slowly. It is confusing while considering the higher k_c, the more radicals captured by micelles or particles, then more particles nucleated. In fact, k_c influences polymerization rate through biradical termination in particles. The faster capture rate the higher probability to termination. It was found that increasing k_c leads to smaller particle size as shown in Fig. 6 and smaller weight average molecular weight (M_w) as shown in Fig. 7. Low value of k_c retards the accumulation of radicals in the particles and thus increases M_w and particle size. There is no experimental parameter available if the total surface of particles used instead of the number of particles in calculating radical capture rate. Radical capture by particles may result in multi-chain in the particles.

3.2.1.2. Rate coefficient for radical desorption. Simulation runs were carried out using different value of desorption rate constant (k_{des}) as shown in Fig. 8. The polymerization rate decreased with increasing k_{des} value. By the same analysis, it was found that increasing k_{des} did not change particle size and its distribution. The effect of k_{des} on M_w is shown in Fig. 9. As k_{des} increased, M_w increased in the low and middle conversion. This may be explained through the number of active particles shown in Fig. 10. As k_{des} increased, the radicals produced by chain transfer to monomer within the particles have larger probability for leaving the particles, which should result in a smaller number of active particles, thus the individual particle have higher monomer concentration which cause higher polymerization rate in the individual particle and higher molecular weight. This also may explain the lower total polymerization rate with larger k_{des} value since polymerization rate is proportion to the number of active particles. Besides, the lower polymerization rate would due to the higher termination caused by desorbed radicals. The slight decrease of M_w as conversion (f) approaches to 1.0 was due to the lack of monomer, which caused termination and formation of oligomers in particles.

From above discussions, we can find the parameters of $k_c=5\times10^5$ M^{-1} s^{-1} which was found experimentally to be in the range of 5×10^5 to 5×10^6 M^{-1} s^{-1} [3] and $k_{des}=8\times10^6$ s^{-1} used as an adjustable parameter to fit the experimental data since its value was not well established experimentally.

3.2.2. Prediction of styrene system

3.2.2.1. Kinetics of polymerization. The rate parameters used in the simulation shown in the caption of Fig. 11 are the same with those used by Guo et al. except k_c and k_{des} as discussed before. The value of k_{tr} available is quite different [3,5], we chose 0.006 as a reasonable one. The monomer loading in the initial microemulsions (M_0) is calculated from the concentration of their components. The simulated

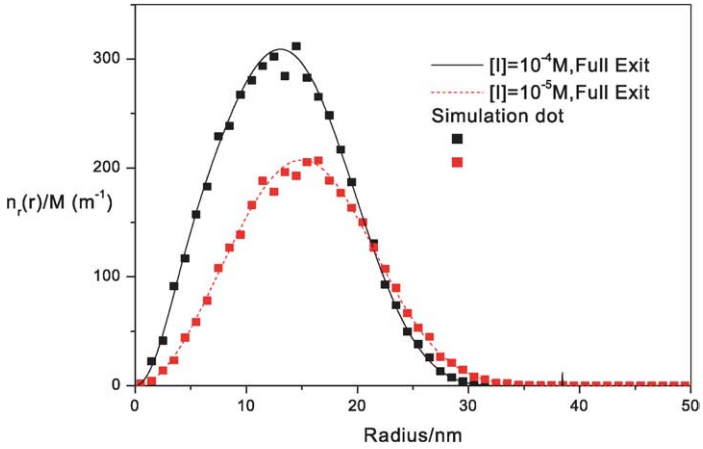

Fig. 3. Particle size distribution at 98% conversion calculated for the full exit case at two initiator concentrations. Parameter values are the same as Fig. 1. Solid lines are theory calculation and dots are simulated results.

kinetic behaviors are shown in Fig. 11, which reproduce the experimental results with different initiator concentration. The maximum in reaction rate (R_{max}) occurs at the same conversion regardless of the concentration of initiator (inset in Fig. 11. The more detail information from simulation results show that biradical termination in particles only counts few percent of total radicals, but termination in aqueous phase is rather serious.

Also, we used the same scheme to simulate the experimental data obtained by Kaler [5] shown in Fig. 12. Though the polymerization temperature is 60 °C, slightly lower than Guo's, we expect the change of the constant value with temperature is very small. We chose the same value of k_c and k_{des}. The initial monomer concentration in polymer particles (C_0) is chosen 5.0 M since the monomer loading in the initial microemulsions (M_0) is 0.254 M, lower than Guo's. The good agreement between simulation and experimental results is obviously, especially in low initiator concentration.

3.2.2.2. Particle nucleation and number of polymer particles. As found by Guo et al., the particle generation rate at the beginning of the polymerization of styrene microemulsions was about the same as the initial primary radical production rate from initiator decomposition [7]. The simulation results are very similar with their findings.

In our scheme, small radicals with enough solubility in aqueous phase could enter and exit a large number of swollen micelles before eventually propagating in one as suggested by Kaler [5]. The probability of desorption of small radicals is very high. The possibilities of homogeneous nucleation were also investigated. The result showed that for such hydrophobic monomer like styrene homogeneous nucleation could be safely ruled out. Fig. 13 shows the number of particles change with time during polymerization. The consistence between simulation and experimental results confirms that our scheme figures out the essential events happening in the polymerization.

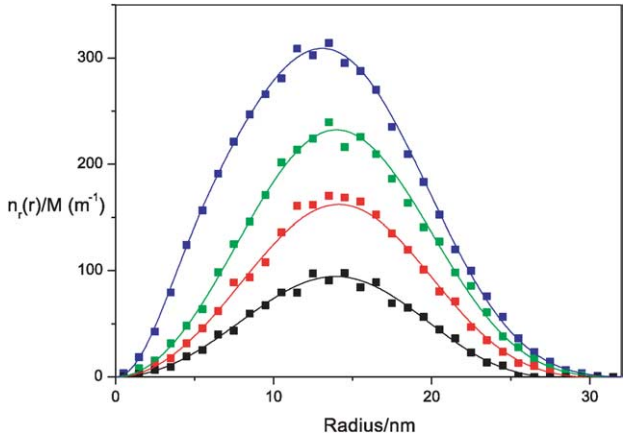

Fig. 4. Evolution of the particle size distribution with conversion in the case of full exit. From bottom to top: 25, 50, 75 and 98% conversion. $[I] = 10^{-4}$ M, and other values are the same as used in Fig. 1. Solid lines are theory calculation and dots are simulated results.

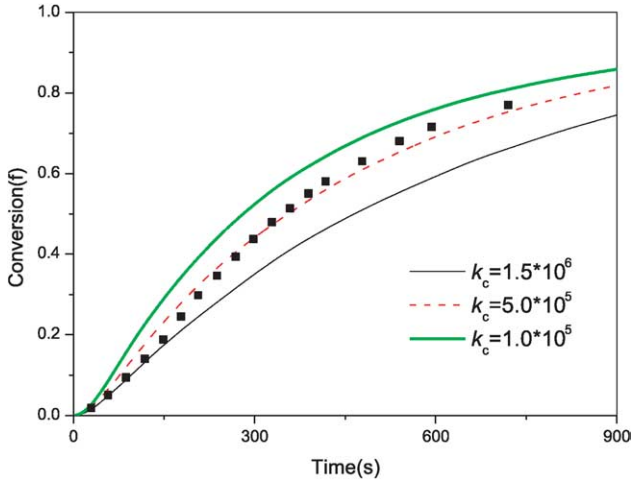

Fig. 5. Model predictions of conversion as a function of time for different values of k_c, and the dots (■) were the experimental data from Fig. 1 in Ref. [3] using 0.27 mM KPS.

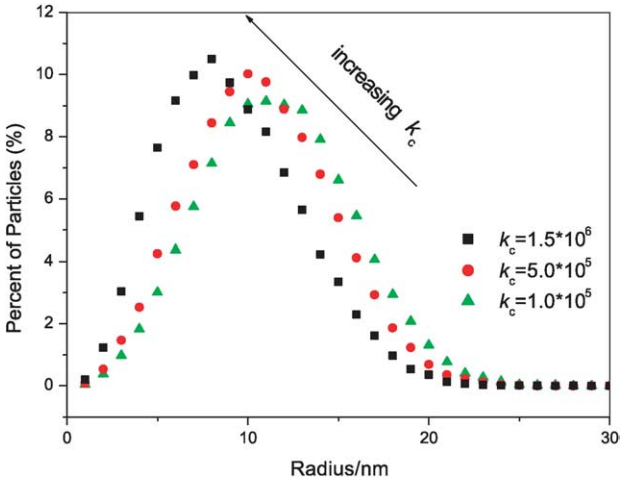

Fig. 6. Simulated number average particle size distributions for polymerized styrene oil-in-water microemulsion latexes with different value of k_c as used in Fig. 5.

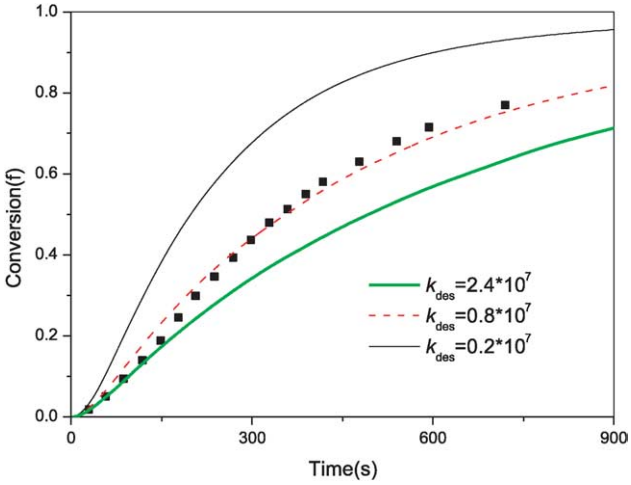

Fig. 8. Model predictions of conversion as a function of time for different values of k_{des}, dots (■) are the same in Fig. 5.

3.2.2.3. Molecular weight distribution and particles size distribution. Fig. 14 shows the simulated molecular weight distributions at varying conversions during styrene microemulsion polymerization. Average molecular weights obtained from the simulation were around several million and remain essentially constant during the course of the reaction, which are sensitive to chain transfer constant since the major termination style is chain transfer to monomer and, to a much smaller extent, biradical termination. The polydispersity indexes of MWD according to the model predicted are about 2.0. This is consistent with the model assumption that radical chains are terminated essentially by disproportionation, which is chain transfer reaction here. Increasing the KPS concentration to 10 times and 100 times to 0.27 mM shifts the molecular weight to lower value as shown in Fig. 15, also as observed by Kaler [12]. The PSDs change with KPS concentration was shown in Fig. 16. The higher the initiator concentration the smaller the particle size. The polydispersity indexes of PSD (ratio of the weight average particle size to number average one) are 1.36, 1.36, 1.42 for 0.27, 2.7, 27 mM run, respectively, like the value obtained by Guo [7].

Fig. 17 shows the number- and weight-based particle size distribution obtained from our model, similar with the experimental results from literatures. The number-average diameter and weight-average diameter were 20.4 and 27.8 nm. The experimental values were 23.3 and 30.3 nm, respectively, [7]. The slight difference is due to the calculation method. In the simulation, diameter was calculated using the polymer weight in the particle and assumed bulk density. However, experimental value accounts for the surfactant layer and the polymers in the small particle always pack more loosely than bulk [23,24].

3.2.3. Prediction of HMA system

The model was used to predict the HMA system choosing parameters of $k_c = 1.0 \times 10^7\ M^{-1}\ s^{-1}$ and $k_{des} = 1.0 \times 10^4\ s^{-1}$.

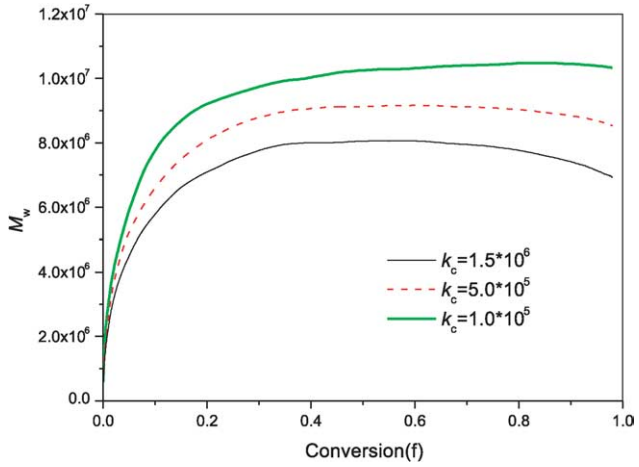

Fig. 7. Simulated weight average molecular weight vs. conversion for polymerized styrene oil-in-water microemulsion latexes with different value of k_c as used in Fig. 5.

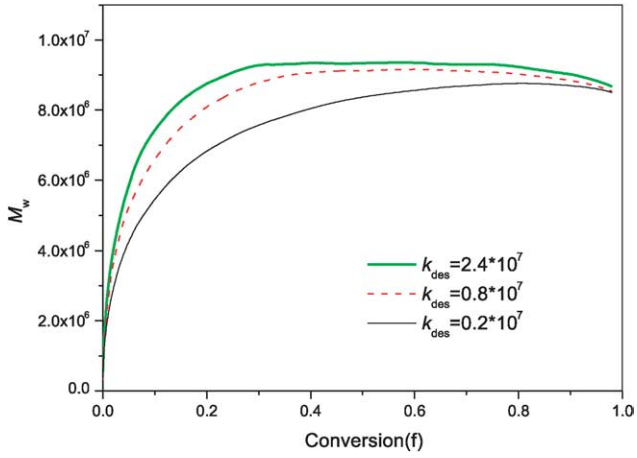

Fig. 9. Simulated weight average molecular weight vs. conversion for polymerized styrene oil-in-water microemulsion latexes with different value of k_{des} as used in Fig. 8.

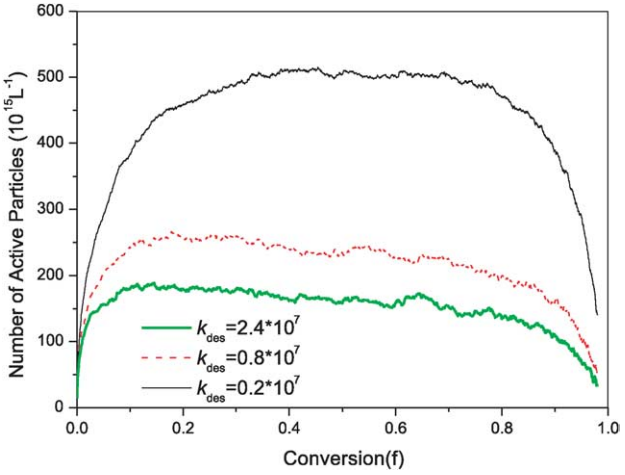

Fig. 10. Simulated number of active particles vs. conversion for polymerized styrene oil-in-water microemulsion latexes with different value of k_{des} as used in Fig. 8.

It is quite reasonable that more hydrophobic monomer will have higher entry rate constant and lower desorption rate constant since the oligmeric radical would like to stay in the hydrophobic environments instead of aqueous phase. The dynamic results are shown in Fig. 18 compared with experimental results. In Ref. [4], slightly different A value (Eq. (6)) were used to obtain a better fit for different initiator concentrations. Since these parameters set should not change with different initiator concentrations, we select the same parameters set for these series of simulations. Though, we can also choose different rate constants to achieve a better fit, it is of no sense. The difference in the low initiator concentration is very likely due to the impurity

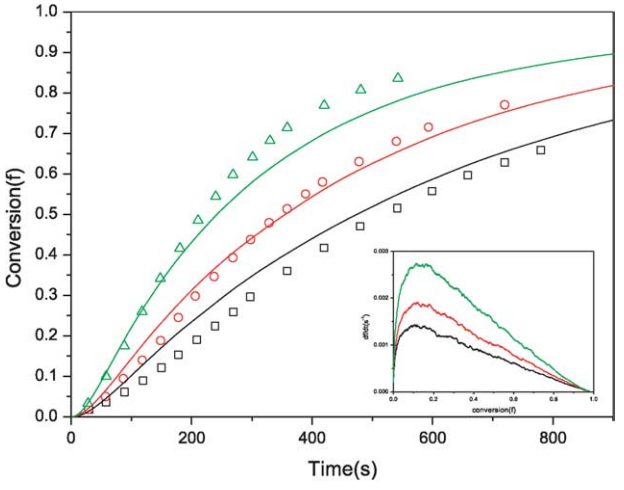

Fig. 11. Simulated conversion (solid line) vs. time for the microemulsion polymerization of styrene at 70 °C. Dots are experimental results from Ref. [3] with different concentration of KPS (△) 0.69 mM, (○) 0.27 mM and (□) 0.14 mM. Inset: predicted polymerization rate as a function of conversion for data shown in the figure. Parameter values used in the simulation are $C_0=7.0$ M, $k_d=4.4\times10^{-5}$ s^{-1}, $k_p=329$ M^{-1} s^{-1}, $M_0=0.466$ M, $k_t=1.07\times10^8$ M^{-1} s^{-1}, $k_c=5\times10^5$ M^{-1} s^{-1}, $k_{des}=8.0\times10^6$ M^{-1} s^{-1}and $k_{tr}=0.006$ M^{-1} s^{-1}.

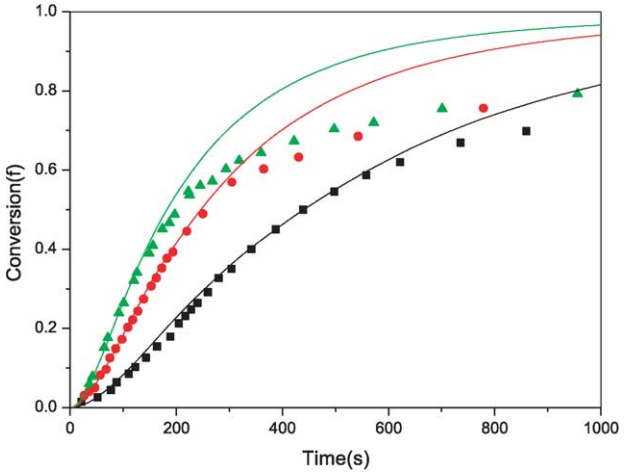

Fig. 12. Simulated kinetics for styrene/DTAB microemulsions (solid line) and experimental data (dots) from Fig. 9 of Ref. [5]. The initiator concentration are (▲) 0.49 mM, (●) 0.24 mM, and (■) 0.061 mM of V-50. Parameter values used in the simulation are $C_0=5.0$ M, $k_d=3\times10^{-5}$ s^{-1}, $k_p=342$ M^{-1} s^{-1}, $M_0=0.254$ M, $k_t=1.07\times10^8$ M^{-1} s^{-1}, $k_c=5\times10^5$ M^{-1} s^{-1}, $k_{des}=8.0\times10^6$ M^{-1} s^{-1}and $k_{tr}=0.006$ M^{-1} s^{-1}.

in the microemulsions, which would retard the polymerization. If we shift the simulation line along the x-axis to a few seconds a good fit would be obtained. We are convinced that the general polymerization behavior of hydrophobic monomer in microemulsions was properly simulated by the model proposed here.

4. Conclusion

A simple Monte Carlo simulation model for the kinetics of microemulsion polymerization is proposed. The properties of final latex such as the particle size and molecular weight distributions can be obtained simultaneously. The agreement between simulation and analytical result as well

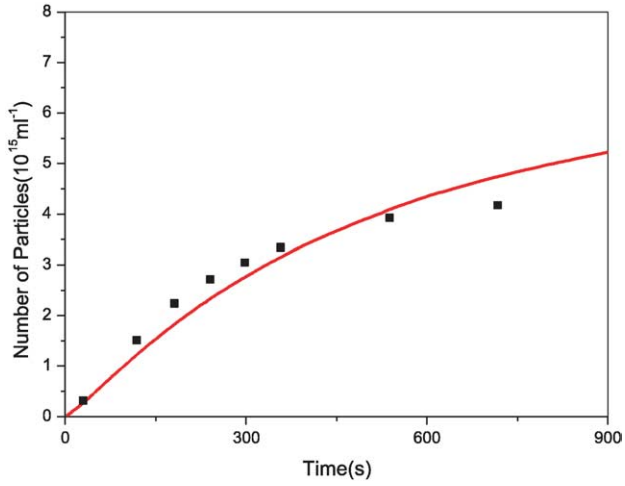

Fig. 13. Experimental results (solid square dots) and model prediction (solid curve) of particle number for styrene microemulsion polymerization with 0.27 mM KPS at 70 °C.

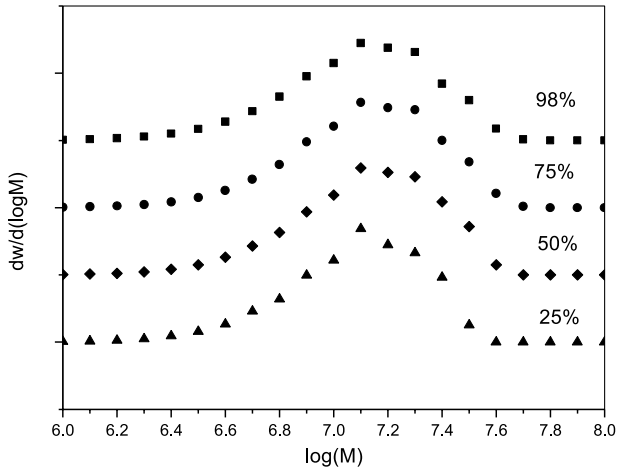

Fig. 14. Variation of the simulated MWDs with conversion for styrene microemulsion polymerization with 0.27 mM KPS at 70 °C.

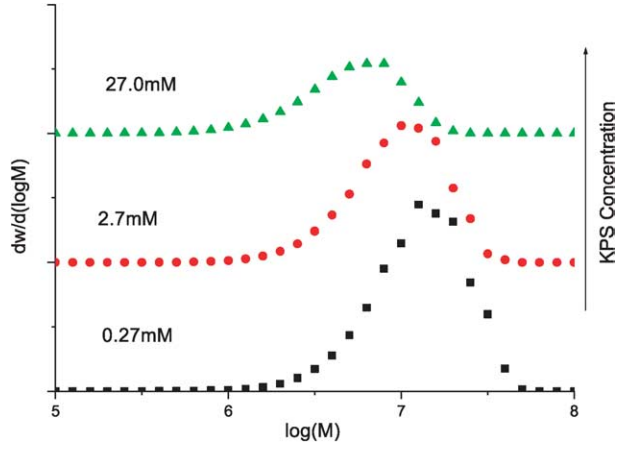

Fig. 15. Variation of the simulated MWDs with KPS concentration for styrene microemulsion polymerization at 70 °C.

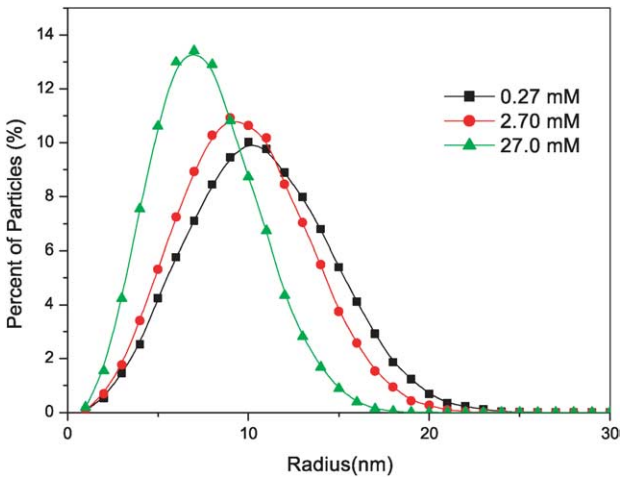

Fig. 16. Variation of the simulated number-based PSDs with KPS concentration for styrene microemulsion polymerization at 70 °C.

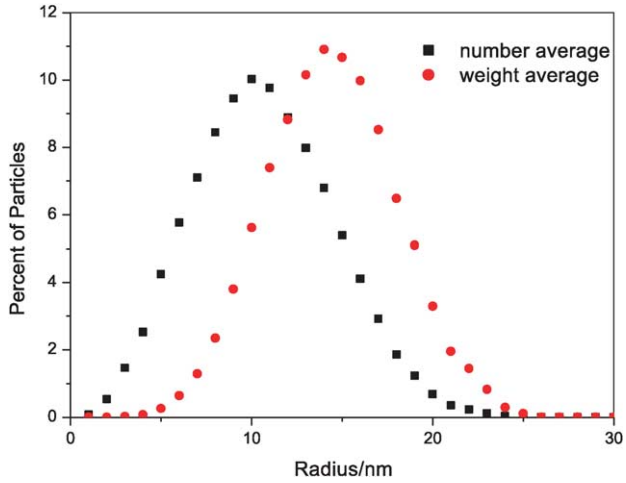

Fig. 17. Simulated number- and weight-based particle size distributions for polymerized styrene oil-in-water microemulsion latexes with 0.27 mM KPS at 70 °C.

as experimental results has been demonstrated. The entry and desorption mechanism was well established to account for the polymerization kinetics of hydrophobic monomer in microemulsions. It is straightforward to account for virtually any kinetic event such as chain length dependence of kinetic parameters, and very detailed information can be obtained since one can observe each polymer chain and each particle as well as their distributions directly. The present simulation method makes it possible to examine the applicability of the mechanistic models directly and will provide greater insight into the complicated phenomena of microemulsion polymerizations. More possible and reasonable events would be introduced into the model and the monomer starvation effect and more general model for microemulsion polymerization are the focus of the current ongoing study.

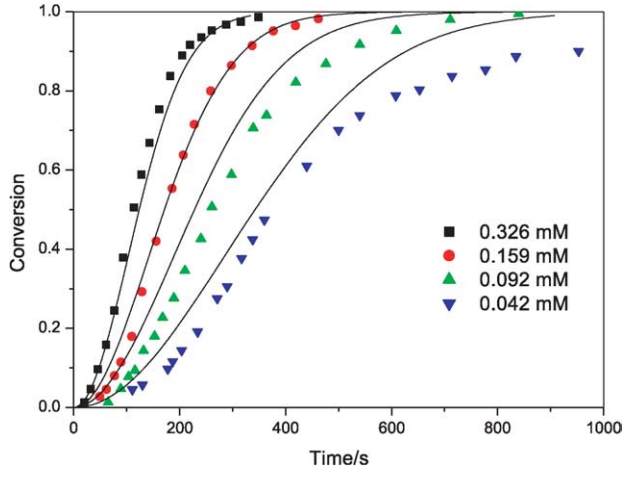

Fig. 18. Simulated conversion vs. time for the microemulsion polymerization of HMA with different V-50 initiator concentration. Dots are experimental results from Fig. 1 in Ref. [4].

Acknowledgements

The authors thank the National Natural Science Foundation of China (20374011) and the Major State Basic Research Development program (G1999064800) for their financial supports. H. Zhang greatly acknowledges the National Special Fund of China for Excellence in PhD Dissertations and 'Shuguang' Project of Shanghai Education Development Foundation.

References

[1] Antonietti M, Tauer K. Macromol Chem Phys 2003;204:207–19.
[2] Meier W. Curr Opin Colloid Interf Sci 1999;4:6–14.
[3] Guo JS, Sudol ED, Vanderhoff JW, El-Aasser MS. J Polym Sci, Polym Chem Ed 1992;30:703–12.
[4] Morgan JD, Lusvardi KM, Kaler EW. Macromolecules 1997;30: 1897–905.
[5] de Vries R, Co CC, Kaler EW. Macromolecules 2001;34:3233–44.
[6] Mendizabal E, Flores J, Puig JE, Lopez-Serrano F, Alvarez J. Eur Polym J 1998;34:411–20.
[7] Guo JS, Sudol ED, Vanderhoff JW, El-Aasser MS. J Polym Sci, Polym Chem Ed 1992;30:691–702.
[8] Maxwell IA, Morrison BR, Napper DH, Gilbert RG. Macromolecules 1991;24:1629–40.
[9] Asua JM, Sudol ED, El-Aasser MS. J Polym Sci, Polym Chem Ed 1989;27:3903–13.
[10] Morgan JD, Kaler EW. Macromolecules 1998;31:3197–202.
[11] Co CC, Kaler EW. Macromolecules 1998;31:3203–10.
[12] Co CC, Cotts P, Burauer S, de Vries R, Kaler EW. Macromolecules 2001;34:3245–54.
[13] Co CC, de Vries R, Kaler EW. Macromolecules 2001;34:3224–32.
[14] Gillespie DT. J Phys Chem 1977;81:2340–61.
[15] Lu JM, Zhang HD, Yang YL. Macromol Theor Simul 1993;2:747–60.
[16] He JP, Zhang HD, Yang YL. Macromol Theor Simul 1995;4:811–9.
[17] He JP, Zhang HD, Chen JM, Yang YL. Macromolecules 1997;30: 8010–8.
[18] Jabbari E. Polymer 2001;42:4873–84.
[19] Chen YC, Chiu WY. Polymer 2001;42:5439–48.
[20] He XH, Liang HJ, Pan CY. Polymer 2003;44:6697–706.
[21] He CX, Costeux S, Wood-Adams P, Dealy JM. Polymer 2003;44: 7181–8.
[22] Nomura M. Emulsion polymerization. New York: Academic Press; 1982. Chapter 5.
[23] Wu C, Chan KK, Woo KF, Qian RY, Li XH, Chen LS, et al. Macromolecules 1995;28:1592–7.
[24] Qian RY, Wu LH, Shen DY, Napper DH, Mann RA, Sangster DF. Macromolecules 1993;26:2950–3.